URN (Paper): urn:nbn:de:gbv:ilm1-2014iwk-101:4

CALIBRATION OF HEAT FLUX SENSORS WITH SMALL HEAT FLUXES

Michael Hohmann, Paul Breitkreutz, Marc Schalles, Thomas Fröhlich

Technische Universität Ilmenau, Institute for Process Measurement and Sensor Technology,
POB 100565, 98684 Ilmenau

ABSTRACT

A new calibration bench was developed at the Institute for Process Measurement and Sensor Technology to calibrate heat flux sensors (HFS). The bench provides well known temperatures at both sides of the HFS, from which the heat flux can be determined. The temperatures are determined using a method known from the calibration of contact surface thermometers. By means of thermocouples inside homogenization blocks, the surface temperatures of the homogenization blocks, and thereby the surface temperatures of the HFS, are extrapolated. The heaters are controlled in a manner that the surface temperatures change from equal values to certain differences. Using these temperature differences and the sensor signal, the offset and the sensitivity of the HFS can be determined.

Index Terms - heat flux sensor, calibration, surface temperature

1. INTRODUCTION

Heat flux sensors (HFS) for heat flux of conductive origin are usually calibrated at calibration benches using the guarded-hot-plate-method [1]. This method requires a known heat flux through the sensor under test, which is usually provided by measuring the temperature difference over a plate with known geometry and thermal conductivity. One of the main requirements for this method is a one-directional heat flux from the heat source to and through the sensor under test, which can only imperfectly be provided. The calibration bench presented in this paper uses a different approach. It uses the determination of the surface temperature of the sensor under test to determine its characteristics.

2. DESIGN AND OPERATING PRINCIPLE

2.1 Calibration bench

The calibration bench is an axial symmetrical construction consisting of two meander-shaped heaters and two homogenization blocks (steel 1.4301) with integrated thermocouples (TCs) type K, surrounded by an insulation made of alkaline-earth silicate wool (Figure 1). The homogenization blocks are 76 mm in diameter and 25 mm in height. The geometry of the air gap between the blocks depends on the geometry of the sensor under test (the HFS). The heaters on top of the upper and at the bottom of the lower homogenization block can be controlled individually. The bench can be operated in a temperature range from 20 °C to 400 °C.

The three TCs in each homogenization block are used to extrapolate to the blocks surface temperature using a quadratic function approach. This method is known from the calibration of contact surface thermometers [2, p. 157]. Using this method, the surface temperatures of the homogenization blocks and of the HFS respectively, are determined and used as controlled variable. The heaters are controlled in a manner that the extrapolated surface

temperatures change from $\Delta T = 0$ K to $\Delta T = \pm 200$ mK. The temperature difference of 200 mK was found to be great enough to get an evaluable signal and small enough to get a not to high deformation of the thermal field.

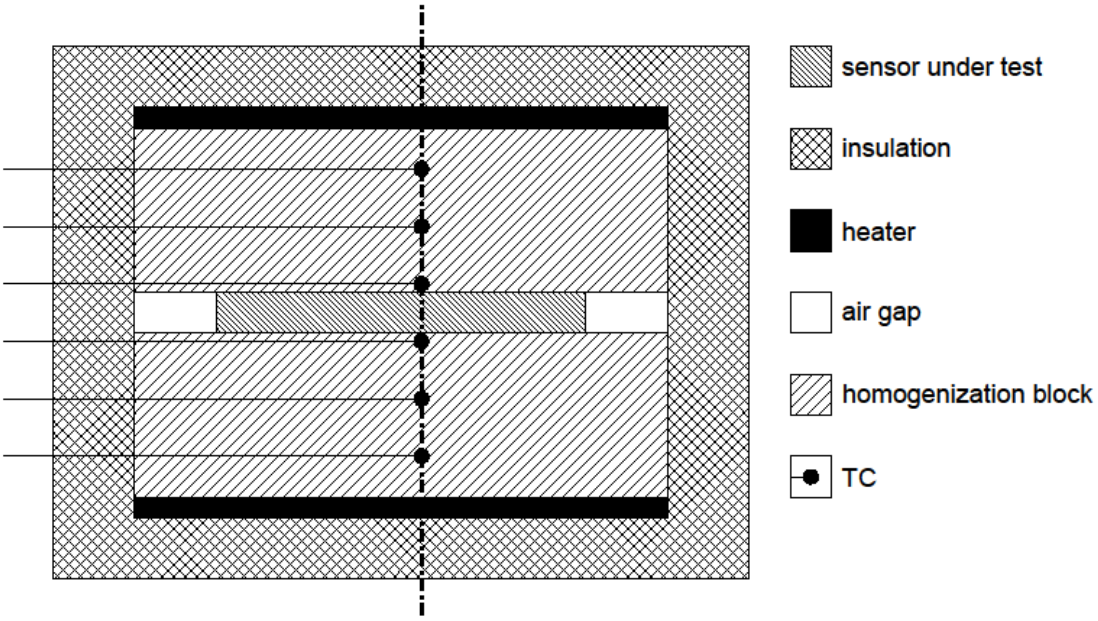

Figure 1: Design of the calibration bench.

The aim of the calibration is to determine the sensitivity S and the offset U_0 of the characteristic (1) of the HFS, where ΔT is the temperature difference between top and bottom of the HFS.

$$U_{\mathrm{HFS}} = U_0 + S \cdot \Delta T \tag{1}$$

Each of the temperatures has errors due to temperature measurement and the unknown temperature field across the surface of the HFS (2).

$$U_{\mathrm{HFS}} = U_0 + S \cdot [(T_{\mathrm{upper}} + E_{\mathrm{upper}}) - (T_{\mathrm{lower}} + E_{\mathrm{lower}})] \tag{2}$$

To compensate the influence of these errors, two different temperature differences T_{upper}-T_{lower} (a and b) are used to determine $S(\Delta T)$. Assuming that the errors E are constant or change negligibly, $S(\Delta T)$ can be determined using the two signals U and the four temperatures T (3).

$$\begin{aligned} U_{\mathrm{A}} &= U_0 + S \cdot [(T_{\mathrm{upper,a}} + E_{\mathrm{upper}}) - (T_{\mathrm{lower,a}} + E_{\mathrm{lower}})] \\ U_{\mathrm{B}} &= U_0 + S \cdot [(T_{\mathrm{upper,b}} + E_{\mathrm{upper}}) - (T_{\mathrm{lower,b}} + E_{\mathrm{lower}})] \\ S(\Delta T) &= \frac{U_{\mathrm{a}} - U_{\mathrm{b}}}{(T_{\mathrm{upper,a}} - T_{\mathrm{lower,a}}) - (T_{\mathrm{upper,b}} - T_{\mathrm{lower,b}})} \end{aligned} \tag{3}$$

To determine the offset U_0, the HFS has to be flipped at one temperature (4).

$$
\begin{aligned}
U_{\text{up}} &= U_0 + S \cdot [(T_{\text{upper}} + E_{\text{upper}}) - (T_{\text{lower}} + E_{\text{lower}})] \\
U_{\text{down}} &= U_0 + S \cdot [(T_{\text{lower}} + E_{\text{lower}}) - (T_{\text{upper}} + E_{\text{upper}})] \\
U_0 &= \frac{U_{\text{up}} + U_{\text{down}}}{2}
\end{aligned} \tag{4}
$$

To get the sensitivity as a function of heat flux $\dot{q}$, the one-dimensional formulation of Fourier's law (5) is used, where λ is the thermal conductivity. With the assumptions of one-dimensional heat conduction and a constant temperature gradient across the length l of the sensor one gets (6).

$$\dot{q} = -\lambda \nabla T \tag{5}$$

$$\dot{q} = -\frac{\lambda}{l} \Delta T \tag{6}$$

Using equations (3) and (6), the sensitivity $S(\dot{q})$ is given by equation (7). The thermal conductivity and the thickness are temperature-dependent, but their changes in the small temperature interval of 200 mK can be neglected.

$$S(\dot{q}) = \frac{l}{\lambda} \cdot \frac{U_{\text{a}} - U_{\text{b}}}{(T_{\text{upper,a}} - T_{\text{lower,a}}) - (T_{\text{upper,b}} - T_{\text{lower,b}})} \tag{7}$$

2.2 Sensors under test

The sensors under test were constructed at the Institute for Process Measurement and Sensor Technology of the Technische Universität Ilmenau to be integrated in a dry block calibrator [5]. The sensors consist of two rings of TCs type E, which are thermally connected in parallel and electrically connected in series. These so called thermopiles have 25 junctions at the inner and 35 junctions at the outer ring and are mounted to a backing made of glass ceramic (54 mm in diameter, 1.5 mm in height) (Figure 2). This construction is based upon a well-known design principle for HFS [3]. Two different designs were constructed, one with and one without filling.

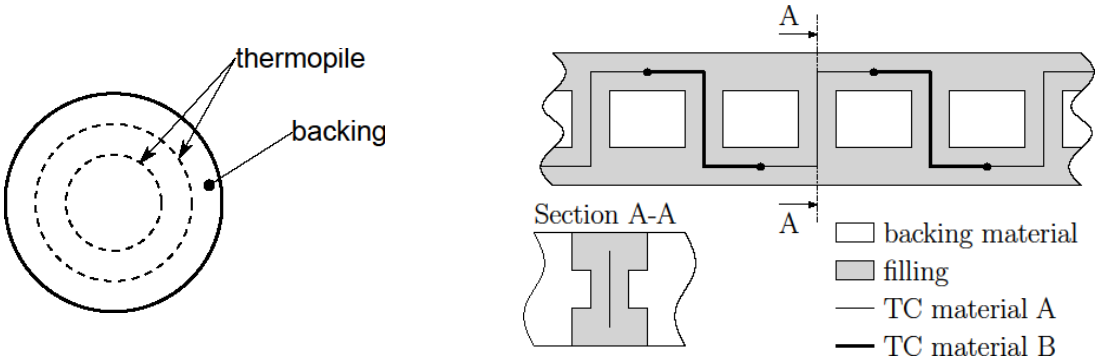

Figure 2: Design of the HFS and cross-section along a thermopile.

The theoretical sensitivity $S(\dot{q})$ (8) depends on the sensitivity $S_{\mathrm{TC}}(T)$ of the TC type E, the distance between the junctions *l*, the thermal conductivity and the number *n* of junctions [3]. The sensitivity $S(\Delta T)$ only depends on $S_{\mathrm{TC}}(T)$ and *n* (9).

$$S(\dot{q}) = \frac{n \cdot S_{\mathrm{TC}}(T) \cdot l}{\lambda} \tag{8}$$

$$S(\Delta T) = n \cdot S_{\mathrm{TC}}(T) \tag{9}$$

To estimate the theoretical sensitivity, the equivalent electrical circuit [2, p. 278] was used. With this model and the values for $S_{\mathrm{TC}}(T)$ from [4] for different temperatures the sensitivity was estimated (Table 1).

Table 1: Theoretical sensitivity of the HFS.

thermopile	60 °C		100 °C		150 °C	
	$S(\Delta T)$ / μVK^{-1}	$S(\dot{q})$ / $\mu VW^{-1}m^2$	$S(\Delta T)$ / μVK^{-1}	$S(\dot{q})$ / $\mu VW^{-1}m^2$	$S(\Delta T)$ / μVK^{-1}	$S(\dot{q})$ / $\mu VW^{-1}m^2$
25 with filling	56.96	406.83	58.61	418.55	60.53	432.26
35 with filling	79.66	568.28	81.96	584.66	84.64	603.81
25 without filling	40.42	194.97	41.59	200.59	42.95	207.16
35 without filling	56.51	272.20	58.14	280.05	60.05	289.22

3. PROPERTIES OF THE BENCH

3.1 Stability of the surface temperatures

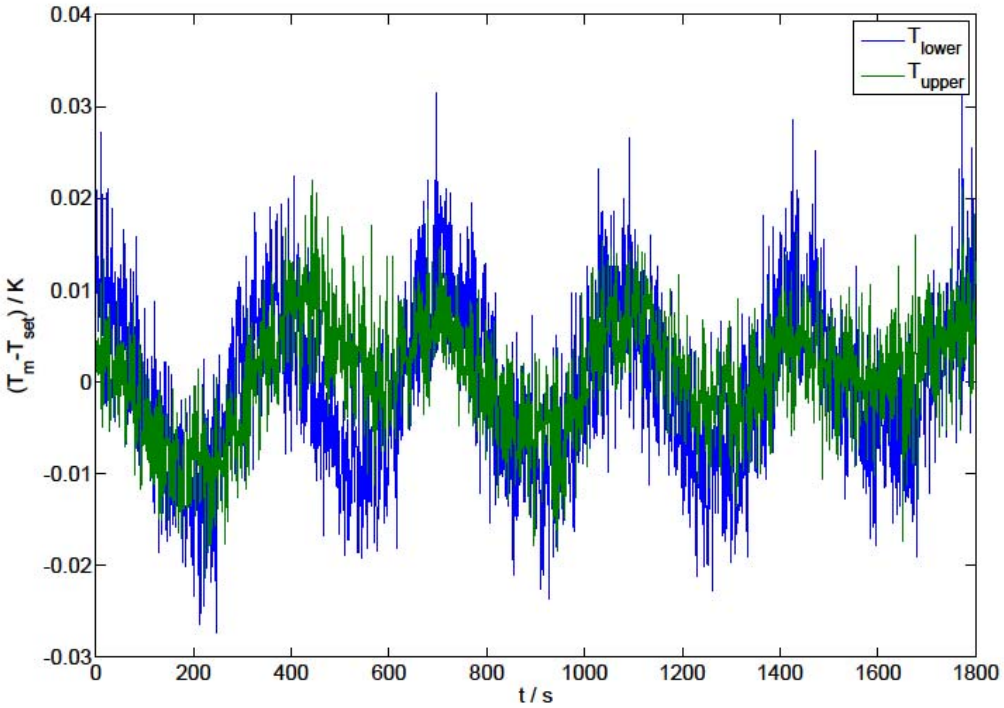

Figure 3: Temperature differences between the setpoint temperature T_{set} and the measured surface temperatures T_{m} of the upper and the lower homogenization block in steady state.

Each of the extrapolated surface temperatures is controlled by a PID-controller respectively. These controllers are able to hold the setpoint, but there are oscillations with a period of about 300 s and a magnitude less than 30 mK around the setpoint (Figure 3). These oscillations are caused by the periodic change of the temperature in the laboratory due to air condition, cross-sensitivity of the two controllers and the nonexistent active cooling. Nevertheless this quality of the controlled temperatures is sufficient for calibration, since integration intervals of 600 s are possible during the calibration process.

3.2 Axial temperature distribution

Figure 4 shows the axial temperature distribution in the blocks during the calibration at T_{set} ~ 100 °C with a temperature difference of T_{upper}-T_{lower} = 100 mK.

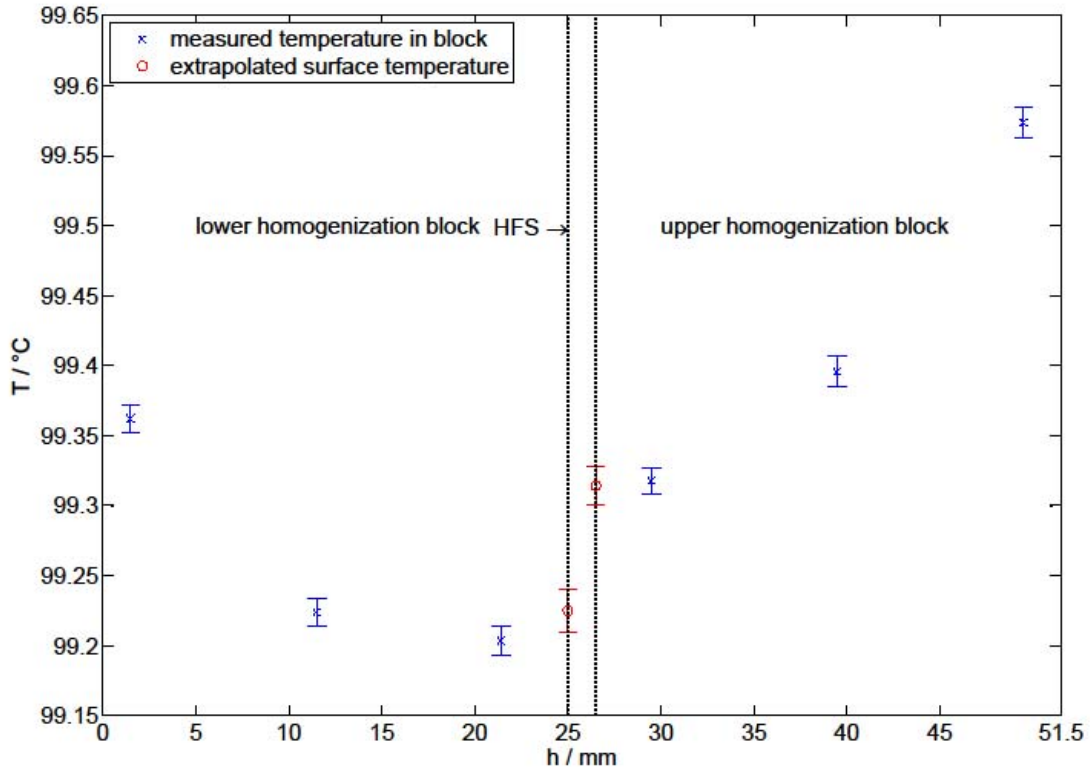

Figure 4: Axial temperature distribution from height h=0 mm *(bottom) to h*=51.5 mm *(top) of the bench at* T_{set} ~ 100 °C *and the temperature difference* T_{upper}-T_{lower} = 100 mK. *The error bars show the standard deviation of the temperatures (2500 data points).*

In each block the temperature distribution follows a quadratic function. The deviation of a linear distribution is caused by the heat exchange with the other block respectively and the heat losses through the insulation. The temperature distribution across both blocks is an indication of high thermal contact resistances between the HFS and the blocks surfaces.

3.3 Homogeneity of the temperature field

To estimate the homogeneity of the temperature field across both sides of the HFS, a TC was used to measure the surface temperatures at several points. For this, a dummy of a HFS with a radial groove was manufactured in which the TC was inserted. For each measurement series, the dummy was rotated 45°. At every angular step, the TC was moved in the groove from the center outwards in 5 mm-steps. This measurement was performed at steady state of the surface temperatures at 60 °C. The results in Figure 5 show, that the absolute temperature difference across the each surface has a magnitude of 160 mK. The deformation of the field

compared to a circular temperature distribution can be explained by the shape of the heaters. Due to the non-uniform heat input, the temperature field gets deformed, which has been simulated with the Finite Element Method (Figure 6). The simulation shows a deformation of the temperature field comparable to the deformation at the measurement (Figure 5).

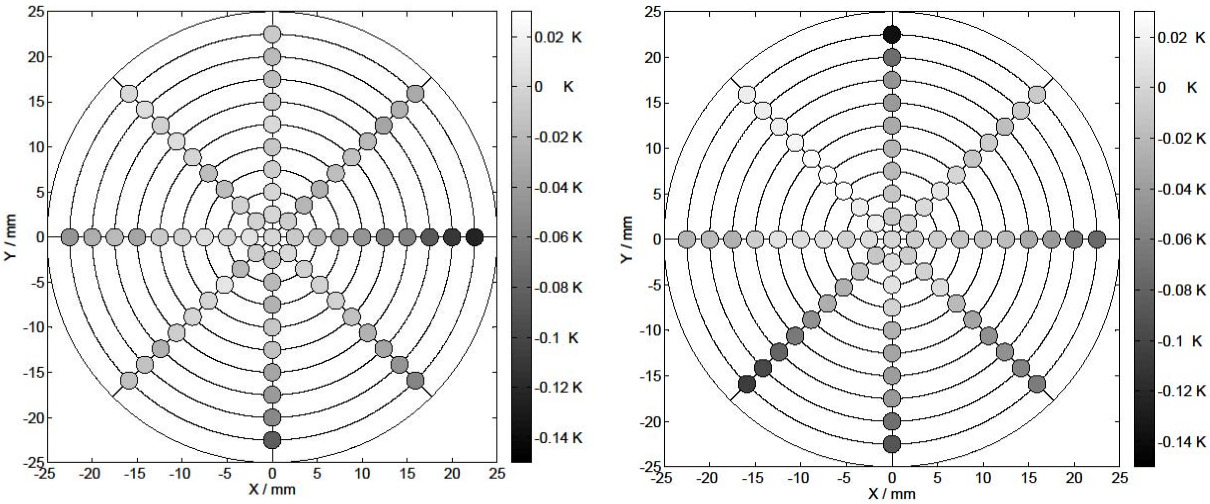

Figure 5: Temperature field at the surface of the upper (a) and the lower (b) homogenization block at T_{set} = 60 °C*, the difference to the extrapolated surface temperature at the center is shown.*

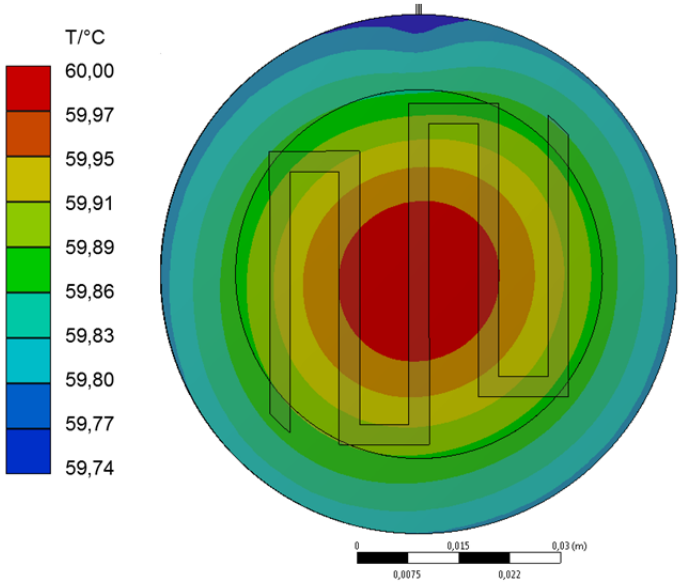

Figure 6: FEM-Simulation of the temperature field due to the non-uniform heat input. The homogenization block, the heater and the position of the HFS are shown.

4. CALIBRATION RESULTS

Due to the long integration interval at every calibration point, the calibration at one temperature takes about 5 h. During this time, 5 calibration points are measured (Figure 7, Figure 8). These points are put in equation (3) in different combinations to get a mean value of the sensitivity.

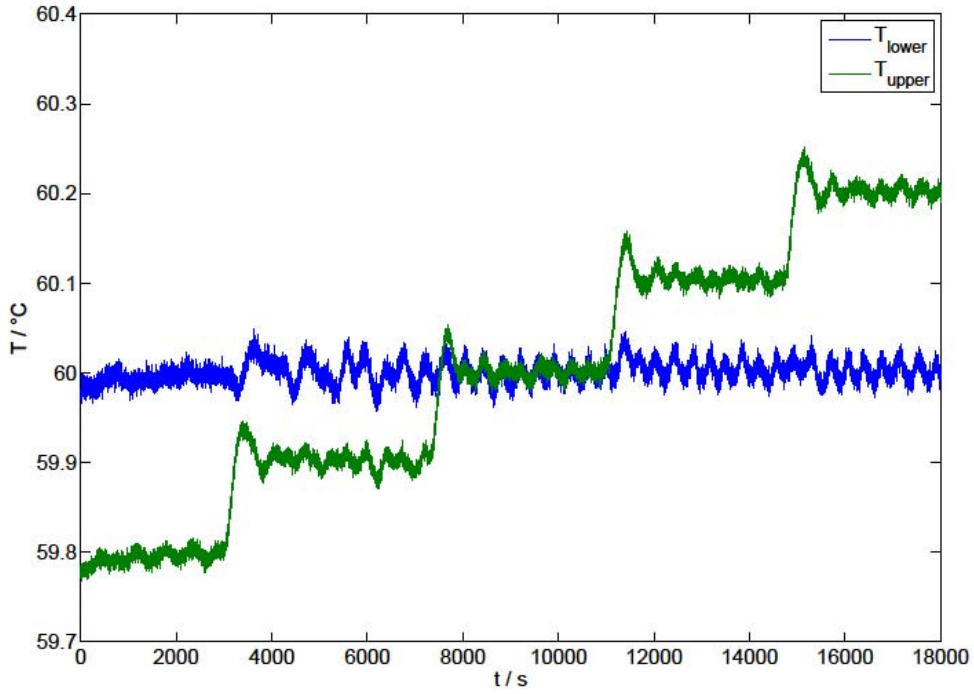

Figure 7: Temperatures during the calibration around 60 °C.

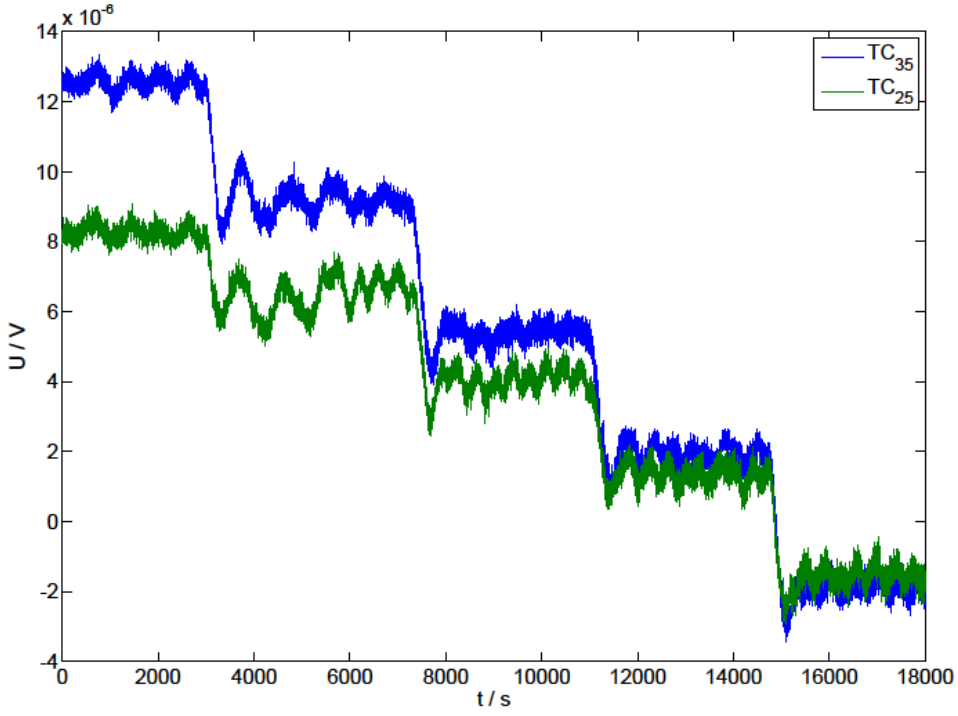

Figure 8: Sensor signals during the calibration around 60 °C.

The high differences between the theoretical values and the measured ones (Table 2) are caused by the thermal resistances between the HFS and the blocks surfaces. These resistances can hardly be measured, but are also present at the real application. Due to this, the measured sensitivities can be used in the application if the surface properties and the contact forces are comparable to the calibration circumstances.

Table 2: Measured sensitivity of the HFS.

thermopile	60 °C		100 °C		150 °C	
	$S(\Delta T)$ / μVK^{-1}	$S(\dot{q})$ / $\mu VW^{-1}m^2$	$S(\Delta T)$ / μVK^{-1}	$S(\dot{q})$ / $\mu VW^{-1}m^2$	$S(\Delta T)$ / μVK^{-1}	$S(\dot{q})$ / $\mu VW^{-1}m^2$
25 with filling	25.52	182.27	28.56	203.95	29.91	213.59
35 with filling	36.63	261.31	36.64	261.37	38.66	275.80
25 without filling	27.19	131.15	30.22	145.75	32.34	155.98
35 without filling	41.14	198.17	46.60	224.43	50.31	242.31

The relative error E_r (10) of the measured sensitivity S_m to the theoretical S_t (Table 3) shows, that the relative error gets smaller with higher temperature and if there is no filling in the HFS. This indicates the influence of the contact resistance. These contact resistances have a higher influence on the sensitivity than the heat conduction trough air or ceramic filler. Additionally, the influence of heat transfer by radiation becomes greater at higher temperatures when there is only air between the thermopiles and the surface of the homogenization blocks.

$$E_r = \frac{S_m - S_t}{S_t} \cdot 100 \tag{10}$$

Table 3: Relative error of the sensitivity.

thermopile	60 °C E_r / %	100 °C E_r / %	150 °C E_r / %
25 with filling	-55.20	-51.27	-50.59
35 with filling	-54.02	-55.30	-54.32
25 without filling	-32.73	-27.34	-24.70
35 without filling	-27.20	-19.85	-16.22

5. CONCLUSION AND OUTLOOK

A new bench for the calibration of heat flux sensors was developed, built up and tested. The thermal properties of the bench like stability of the temperature and axial and radial temperature distribution were measured. The results show, that the bench can be used to calibrate HFS with small heat fluxes. The measured sensitivities compared to the theoretical ones show that every measurement with a HFS has to be checked carefully due to thermal contact resistances. A first set of calibrations from 60 °C to 150 °C has already been carried out, the test with temperatures up to 400 °C is in progress.

6. ACKNOWLEDGEMENTS

The authors would like to thank the German Federal Ministry of Education and Research (BMBF) for the financial support of the VIP-Project “TempKal”, in which context this calibration bench was developed.

REFERENCES

[1] Arpino, F. et al.: Design of a Calibration System for Heat Flux Meters. In: International Journal of Thermophysics 32 (2011), No. 11-12, p. 2727-2734

[2] Bernhard, F. (Ed.): Technische Temperaturmessung. Berlin : Springer-Verlag, 2004

[3] Childs, P. R. N. et al.: Heat flux measurement techniques. In: Proceedings of the Institution of Mechanical Engineers, Part C: Journal of Mechanical Engineering Science (1999), p. 655-677

[4] DIN EN 60584-1: Thermopaare. Teil 1: Grundwerte der Thermospannung (1996)

[5] Hohmann, M. et al.: Metall-Blockkalibrator mit Wärmestromsensoren und adiabatischem Schild. Sensoren und Messsysteme 2014: Beiträge der 17. GMA/ITG-Fachtagung. Berlin : VDE-Verlag, 2014

CONTACTS

M. Sc. Michael Hohmann michael.hohmann@tu-ilmenau.de
Prof. Dr.-Ing. habil. Thomas Fröhlich thomas.froehlich@tu-ilmenau.de